

# On the Gamma Ray Burst Origin of Extremely Energetic Cosmic Rays

Nayantara Gupta <sup>1</sup>

Department of Physics, Indian Institute of Technology Bombay, Powai, Mumbai 400 076, India

## Abstract

Air shower experiments have detected cosmic ray events of energies upto 300 EeV. Most likely these cosmic rays have originated from compact objects. Their exact sources are yet to be identified. It has been suggested before that gamma ray bursts are possible sources of ultra-high energy cosmic rays. The two models of gamma ray burst emissions most often discussed are the internal and external shock models. We have calculated the proton spectrum above 60EeV from all gamma ray bursts distributed upto a redshift of 0.02 in the internal shock model assuming redshift and luminosity distributions consistent with observations, log normal distributions for their values of Lorentz factors, variability times and duration of bursts. Within the external shock model we have calculated the proton flux above 60EeV from all nearby gamma ray bursts assuming log normal distributions in their values of total energies, Lorentz factors at the deceleration epoch and compared with the observed data. We find that gamma ray bursts can produce cosmic ray proton flux comparable to the flux observed by the Pierre Auger experiment both within the internal and external shock models. We have also studied the dependence of the maximum proton energies and the cooling breaks in the proton spectrum on the various parameters like Lorentz factor, energy of the GRB fireball, variability time (in case of internal shocks), ambient particle density (in case of external shocks). Our results are important to understand how the various observable parameters determine which mechanism e.g.  $p\gamma$  interactions, synchrotron cooling of protons will dominate over one another inside these sources.

PACS numbers:98.70.Rz, 98.70 Sa

Keywords: gamma ray bursts, cosmic rays

## 1 Introduction

The field of ultra-high energy cosmic rays (UHECR) enriched with the recent data from the Pierre Auger (PA) experiment [1] has emerged as a very exciting area of research. The highest energy cosmic ray event so far observed was of energy 300EeV, detected by Fly's Eye experiment [2]. Subsequently, many events of energies more than tens of EeV were detected by AGASA [3] and PA experiments. The origin of these extremely energetic cosmic ray events has been investigated since their detection. The current data from PA experiment shows anisotropy and the signature of GZK cut-off [4, 5]. Powerful cosmic ray accelerators *e.g.* gamma ray bursts (GRBs) and active galactic nuclei (AGN) within 200Mpc from us are likely sources of the events detected above the GZK cut-off energy [6]. A possible correlation of the AGN within 75Mpc with the cosmic ray events above 60 EeV has been identified by the PA collaboration [7]. Protons can be accelerated to above 100 EeV within GRBs both

---

<sup>1</sup>nayan@phy.iitb.ac.in

in the internal shock [8, 9] and external shock scenarios [10, 11]. It was suggested by [8] that if all GRBs emit  $5 \times 10^{50}$  erg in cosmic rays and the spectral index ( $p$ ) of the accelerated proton spectrum ( $dN/dE \propto E^{-p}$ ) inside them is  $p \leq 2$  then they can explain the observed UHECR spectrum. The association of GRBs with UHECR has been further discussed in [9]. The energy production in cosmic rays was assumed to be same as the energy production in photons of energy between 20keV-2MeV which was used as  $2 \times 10^{53}$  erg in this calculation and spectral index of proton spectrum  $p = 2$ . The local star formation rate was folded with the maximum distance from which GRBs can contribute to the observed proton spectrum at a particular energy and the proton spectrum from individual GRBs to calculate the diffuse proton spectrum. GRBs were identified as possible origin of ultra high energy cosmic rays. Within the external shock model it was shown that GRBs can explain the observed UHECR spectrum assuming all GRBs emit an average energy  $3.3 \times 10^{53}$  erg in cosmic rays and proton spectral index  $p = 2.2$ . Although a steeper spectrum gave a better fit for the data below  $10^{19}$  eV but due to the contributions of Galactic cosmic rays this fit can not be considered as better. Ultra-high energy (UHE) heavy nuclei can survive from photo-disintegration in the intense photon fields of GRBs in case of external shocks. It may also be possible in case of internal shocks if the shocks occur at relatively large radii [12].

A few low luminosity (LL) GRBs have been detected before *e.g.* GRB 060218/SN 2006aj and GRB 980425/SN 1998bw at redshifts of 0.033 and 0.0085 respectively. These GRBs show some common characteristics like long duration, low isotropic  $\gamma$ -ray energy and low luminosity. Their detections at very low redshifts within a comparatively short period of time imply that they are much more frequent than the canonical HL GRBs [13, 14, 15, 16]. The emission of UHE heavy nuclei and protons from high and low luminosity (HL and LL) GRBs have been studied by Murase et al. [17] considering internal and external shocks. HL and LL GRBs can emit UHE protons and heavy nuclei within the shock scenarios considered in their paper. Within the internal shock scenario LL GRBs are unlikely to produce 100 EeV protons but they can produce 100 EeV heavy nuclei. The values of the GRB parameters *e.g.* luminosity, Lorentz factor, variability time determine the maximum energy of the cosmic ray particles produced.

The Galactic and extragalactic magnetic fields distort the trajectories of the charged particles and tracing the origin of these particles becomes very complicated. The magnetic fields are poorly known. For protons above 60 EeV the deflection in regular Galactic magnetic field is expected to be about few degrees [7]. For Fe nuclei of same energy the deflection would be 26 times higher. The intergalactic magnetic field has been only measured at the centers of rich galaxy clusters. It can produce deflections from negligible [18] to very large values [19]. For coherence length of about 1 Mpc the intergalactic magnetic field may produce root-mean-square deflection of few degrees for protons of energy 60 EeV traversing through 100 Mpc [7]. As it is more difficult to track the heavy nuclei due to their large deflections, the protons of energy more than 60 EeV are only considered in this paper. Modeling of gamma ray bursts has remained as one of the most challenging problems in theoretical astrophysics for the last three decades. Although, lot of progress has been made in the past few years, as of now there is no unique model for GRBs which can explain all aspects and characteristics of GRB emissions in different wavelengths. The leading models for emission from these sources are the internal and the external shock models [20]. We calculate the proton fluxes from all GRBs within the internal shock scenario using distribution functions for their values of

luminosities, redshifts, Lorentz factors etc. The luminosity distribution functions of GRBs have been used from [16] and for redshift distribution we use star formation rate from [21]. The Lorentz factors, variability times and burst durations are represented by log normal distribution functions [22]. Considering the external shock model the time dependent and time averaged proton fluxes have been calculated. Our calculated fluxes have been compared with observed data on UHECR.

## 2 UHECR Propagation and Spacial Distribution

Cosmic rays produced from a point source are expected to reach us much later compared to the photons due to their deflections by the Galactic and intergalactic magnetic fields [23, 24]. If the cosmic ray protons are randomly scattered in magnetic field  $B$  of coherence length  $\lambda$  then the typical deflection angle is  $\theta \sim (D/\lambda)^{0.5}\lambda/R_L$ , where  $D$  is the distance of the source,  $R_L = E_p/eB$  is Larmour radius. The time delay of cosmic rays can be expressed as  $\tau(E) \sim D\theta^2/4c$ . The dispersion in deflection angle  $\Delta\theta$  gives a dispersion in time delay of protons  $\Delta\tau(E_p)$ . If the dispersion in deflection angle  $\Delta\theta \ll \theta$  then the dispersion in time delay is  $\Delta\tau(E) \ll \tau(E)$ . In this case only a few HL GRB events are expected during  $\Delta\tau(E_p)$ . The extremely energetic cosmic ray events from these GRBs will be spacially localized in a small region which is not consistent with the current data from PA experiment. The proton flux from a GRB in observer's frame is

$$\frac{dN_p^{ob}(E_p^{ob})}{dE_p^{ob}} = \frac{dN_p(E_p)}{dE_p} \frac{(1+z)\cos^2\theta_a}{4\pi D^2} \times \exp(-D/[\cos\theta_a r_\pi(E_p, z)]) \quad (1)$$

where  $E_p^{ob} = E_p/(1+z)$  has been used. We are assuming an average deflection of  $\theta_a$  of the cosmic ray protons above 60 EeV. The comoving radial distance of the GRB is

$$D = \int_0^z \frac{c}{H_0} \frac{dz'}{\sqrt{\Omega_\Lambda + \Omega_m(1+z')^3}} \quad (2)$$

with  $\Omega_\Lambda = 0.73$ ,  $\Omega_m = 0.27$  and the Hubble constant  $H_0 = 71 \text{ km sec}^{-1} \text{ Mpc}^{-1}$ . Due to deflection in magnetic field the average distance traversed by the protons is  $D/\cos\theta_a$ . The ultra-high energy (UHE) protons lose energy during their propagation due to photopion, photopair production. The mean free path of energy loss of an UHE proton with energy  $E_p$  is [6, 25]

$$r_\pi(E_p, z) = (1+z)^{-3} \frac{13.7 \exp[4/E_{p,20}]}{[1 + 4/E_{p,20}]} \text{ Mpc} \quad (3)$$

where  $E_{p,20} = E_p(eV)/10^{20}eV$ . The proton flux from a GRB per unit energy and per unit time is

$$\frac{dN_p^{ob}(E_p)}{dE_p^{ob} dt_p^{ob}} = \frac{dN_p(E_p)}{dE_p \Delta\tau(E_p)} \frac{(1+z)\cos^2\theta_a}{4\pi D^2} \times \exp(-D/[\cos\theta_a r_\pi(E_p, z)]) \quad (4)$$

All the GRBs happening during  $\Delta\tau(E_p)$  contribute to the diffuse cosmic ray flux and the factor  $\Delta\tau(E_p)$  cancels out in the final expression of the diffuse flux.

### 3 The Different Time Scales, Cooling Break and Maximum Energies of Protons

We define the relevant time scales which can be used to calculate the break energy in the shock accelerated proton spectrum and the maximum energies of protons. The wind expansion time scale or dynamical time scale is defined as  $t'_{dyn} = \frac{r}{\Gamma c}$  where  $r$  is the radius of expansion and  $\Gamma$  is the bulk Lorentz factor. The synchrotron cooling time scale of protons in the comoving frame is  $t'_{syn} = \frac{6\pi m_p^2 c^3}{\beta_p'^2 \sigma_{p,T} E_p B'^2}$  where the ratio of speed of protons to that of light is  $\beta_p' \sim 1$ ,  $B'$  is the magnetic field in the comoving frame and  $\sigma_{p,T}$  is the Thomson scattering cross section for protons. The cooling time scale due to  $p\gamma$  interactions is  $t'_{p\gamma} = \frac{r}{\Gamma c f_\pi(E_p)}$ . From the condition  $t'_{dyn} = t'_{syn}$  we get the break energy in the proton spectrum due to synchrotron cooling  $E'_{p,c,syn}$ . The break energy due to  $p\gamma$  interactions  $E'_{p,c,p\gamma}$  can be calculated from  $t'_{dyn} = t'_{p\gamma}$ . The cooling break energy in the shock accelerated proton spectrum is close to the minimum of these two breaks

$$E'_{p,c} = \min[E'_{p,c,syn}, E'_{p,c,p\gamma}] \quad (5)$$

The protons are shock accelerated in magnetic field by Fermi mechanism. Their acceleration time scale is  $t'_{acc} = \frac{2\pi\zeta E'_p}{eB'c}$  where  $\zeta \sim 1$ . If we compare  $t'_{acc}$  with  $t'_{dyn}$ ,  $t'_{syn}$  and  $t'_{p\gamma}$  we get the cut-off energies in the proton spectrum  $E'_{p,max,dyn}$ ,  $E'_{p,max,syn}$  and  $E'_{p,max,p\gamma}$  respectively. The minimum of these three gives the maximum energy of the shock accelerated protons.

$$E'_{p,max} = \min[E'_{p,max,syn}, E'_{p,max,p\gamma}, E'_{p,max,dyn}] \quad (6)$$

### 4 Proton Spectrum in the Internal Shock Model

The internal shock model of prompt emission is widely discussed in the literature [26, 27, 28, 29, 30, 31, 32, 33]. Its most successful aspect is its ability to model the complex temporal profiles of light curves during GRB prompt emission. The observed temporal behaviour reflects the temporal behaviour of the central engine. For long bursts the central engine is located deep inside a collapsing star, whose envelop may act as an additional agent to regulate the variability of the relativistic flow. Relativistically moving shells with Lorentz factors  $\Gamma \sim 100 - 1000$  emerge from the core. The faster moving shell catches up the slower one. When the shells collide with each other their kinetic energy is transformed into internal energy of the fireball. Electrons and protons are shock accelerated in irregular magnetic fields when the shells collide. The total energy of the fireball is distributed among the electrons, protons and the magnetic field where  $\epsilon_e$ ,  $\epsilon_p$  and  $\epsilon_B$  denote the equipartition parameters respectively. The relativistic electron/proton spectra can be represented by broken power laws

$$\frac{dN_x(E'_x)}{dE'_x} \propto \begin{cases} E'_x{}^{-p} & E'_{x,m} < E'_x < E'_{x,c} \\ E'_x{}^{-p-1} & E'_{x,c} < E'_x \end{cases} \quad (7)$$

in the case of slow cooling where  $x = e, p$  for electrons and protons respectively.  $E'_{x,m}$  denotes the minimum injection energy of electrons or protons.  $E'_{e,m} = m_e c^2 \bar{\gamma}'_p g(p) \frac{m_p}{m_e} \frac{\epsilon_e}{\epsilon_p}$  and

$E'_{p,m} = \bar{\gamma}'_p m_p c^2 g(p)$  where  $g(p) = \frac{p-2}{p-1}$  for  $p \gg 2$  and  $g(p) \sim 1/6$  for  $p = 2$  [33].  $\bar{\gamma}'_p \sim 1$ . The cooling break energy is denoted by  $E'_{x,c}$ . We have derived its expression by comparing the dynamical expansion time scale ( $t'_{dyn}$ ) with the cooling time scale ( $t'_{cool}$ ). We use the general expression for  $f_\pi(E_p)$  from [22]

$$f_\pi(E_p) = f_0 \begin{cases} \frac{1.34^{\alpha_2-1}}{\alpha_2+1} \left(\frac{E_p}{E_{pb}}\right)^{\alpha_2-1} & E_p < E_{pb} \\ \frac{1.34^{\alpha_1-1}}{\alpha_1+1} \left(\frac{E_p}{E_{pb}}\right)^{\alpha_1-1} & E_p > E_{pb} \end{cases} \quad (8)$$

Variability time, peak energy of the low energy (KeV-MeV) photon fluence in MeV and corresponding threshold energy of protons for  $p\gamma$  interactions are denoted by  $t_v$ ,  $E_{\gamma,peak,MeV}$  and  $E_{pb}$  respectively.  $\alpha_2 = (p+2)/2$  is the spectral index of the low energy photon spectrum above the peak energy  $E_{\gamma,peak,MeV}$  and below it  $\alpha_1 = (p+1)/2$  (slow cooling).

$$f_0^{HL} = \frac{0.729 L_{\gamma,51}}{\Gamma_{2.5}^4 t_{v,-2} E_{\gamma,peak,MeV}} \frac{1}{\left[\frac{1}{\alpha_2-2} - \frac{1}{\alpha_1-2}\right]}$$

$$f_0^{LL} = \frac{0.729 L_{\gamma,47}}{\Gamma_1^4 t_{v,2} E_{\gamma,peak,keV}} \frac{1}{\left[\frac{1}{\alpha_2-2} - \frac{1}{\alpha_1-2}\right]} \quad (9)$$

where  $r = \Gamma^2 c t_v$  has been used. The magnetic field in the comoving frame inside HL and LL GRBs can be expressed as [34]

$$B'^{HL} = 5 \times 10^4 \text{G} \frac{(\xi_1 \epsilon_{B,-1} L_{tot,51})^{1/2}}{\Gamma_{2.5}^3 t_{v,-2}}$$

$$B'^{LL} = 1.5 \times 10^3 \text{G} \frac{(\xi_1 \epsilon_{B,-1} L_{tot,47})^{1/2}}{\Gamma_1^3 t_{v,2}} \quad (10)$$

where  $\xi$  is the compression ratio, which is about 7 for strong shocks. Comparing  $t'_{dyn} = \frac{r}{\Gamma c}$  and  $t'_{syn} = \frac{6\pi m_p^2 c^3}{\beta_p'^2 \sigma_{p,T} E_p B'^2}$  the cooling break due to synchrotron emission can be derived

$$E'_{p,c,syn} = \frac{1}{t_v} \frac{3m_p^2 c^4}{4\sigma_{p,T} \beta_p'^2 c U \epsilon_B}$$

$$E_{p,c,syn}^{HL} = 2 \times 10^{19} \frac{\Gamma_{2.5}^6 t_{v,-2}}{\xi_1 \epsilon_{B,-1} L_{tot,51}} eV$$

$$E_{p,c,syn}^{LL} = 2 \times 10^{18} \frac{\Gamma_1^6 t_{v,2}}{\xi_1 \epsilon_{B,-1} L_{tot,47}} eV \quad (11)$$

where  $\beta_p' \sim 1$ .

From  $t'_{dyn} = t'_{p\gamma}$  one gets

$$E'_{p,c,p\gamma} = \frac{E_{pb}^{HL,LL}}{1.34} \left[ \frac{E_{pb}^{HL,LL}}{f_0^{HL,LL}} \right]^{1/(\alpha_1-1)}$$

$$E_{pb}^{HL} = 3 \times 10^{16} \frac{\Gamma_{2.5}^2}{E_{\gamma,peak,MeV}} eV$$

$$E_{pb}^{LL} = 3 \times 10^{16} \frac{\Gamma_1^2}{E_{\gamma,peak,keV}} eV \quad (12)$$

The luminosity emitted in synchrotron radiation by electrons is

$$L_\gamma = \frac{\eta_e \epsilon_e}{1 + Y_e} L_{tot} \quad (13)$$

$L_{tot}$  is the total luminosity of the GRB fireball. The radiation efficiency of electrons  $\eta_e = [(E'_{e,c}/E'_{e,m})^{2-p}, 1]$  for slow, fast cooling respectively. The relative importance between inverse compton (IC) and synchrotron cooling of electrons is denoted by

$$Y_e = \frac{L_{e,IC}}{L_{e,syn}} = \frac{-1 + \sqrt{1 + 4\eta_e \epsilon_e / \epsilon_B}}{2} \quad (14)$$

where  $L_{e,IC}$  and  $L_{e,syn}$  (this is same as  $L_\gamma$  in our discussion) are the luminosities of radiations by IC and synchrotron mechanisms respectively. The proton flux in the source rest frame can be normalised as follows

$$\int_{E_{p,min}}^{E_{p,max}} E_p \frac{dN_p(E_p)}{dE_p} dE_p = \epsilon_p E_{tot} \quad (15)$$

$E_{p,min} = \Gamma E'_{p,m}$  is the minimum injection energy in the source rest frame.  $E_{tot}$  is the total energy of the fireball in the same frame. The maximum energy of protons derived by comparing the acceleration and cooling (synchrotron and  $p\gamma$  interaction) time scales are  $E'_{p,max,syn}$ ,  $E'_{p,max,p\gamma}$  respectively.

$t'_{acc} = \frac{2\pi\zeta E'_p}{eB'c} = t'_{syn}$  and  $\zeta \sim 1$  give

$$\begin{aligned} E_{p,max,syn}^{HL,LL} &= \Gamma \left[ \frac{3m_p^2 c^4 e}{\sigma_{p,T} \beta_p'^2 B'} \right]^{0.5} \\ E_{p,max,syn}^{HL} &= 10^{20} \Gamma_{2.5}^{5/2} \left[ \frac{t_{v,-2}}{(\xi_1 \epsilon_{B,-1} L_{tot,51})^{1/2}} \right]^{1/2} eV \\ E_{p,max,syn}^{LL} &= 6 \times 10^{19} \Gamma_1^{5/2} \left[ \frac{t_{v,2}}{(\xi_1 \epsilon_{B,-1} L_{tot,47})^{1/2}} \right]^{1/2} eV \end{aligned} \quad (16)$$

and  $t'_{acc} = t'_{p\gamma}$  gives

$$E_{p,max,p\gamma} = \Gamma \left[ \frac{1 + \alpha_1}{f_0} \frac{eB'c\Gamma t_v}{2\pi\zeta} \left( \frac{E'_{pb}}{1.34} \right)^{\alpha_1 - 1} \right]^{1/\alpha_1} \quad (17)$$

For,  $\alpha_1 = 1.5$

$$\begin{aligned} E_{p,max,p\gamma}^{HL} &= 8 \times 10^{18} \left[ \frac{\xi_1 \epsilon_{B,-1} L_{tot,51}}{E_{\gamma,peak,MeV} f_0^{HL2}} \right]^{1/3} eV \\ E_{p,max,p\gamma}^{LL} &= 3.6 \times 10^{18} \left[ \frac{\xi_1 \epsilon_{B,-1} L_{tot,47}}{E_{\gamma,peak,keV} f_0^{LL2}} \right]^{1/3} eV \end{aligned} \quad (18)$$

The maximum energy derived by comparing the acceleration and dynamical time scales is

$$\begin{aligned}
E_{p,max,dyn}^{HL,LL} &= \frac{eB'c\Gamma^2 t_v}{2\pi} \\
E_{p,max,dyn}^{HL} &= 6 \times 10^{19} \frac{(\xi_1 \epsilon_{B,-1} L_{tot,51})^{1/2}}{\Gamma_{2.5}} eV \\
E_{p,max,dyn}^{LL} &= 2 \times 10^{19} \frac{(\xi_1 \epsilon_{B,-1} L_{tot,47})^{1/2}}{\Gamma_1} eV
\end{aligned} \tag{19}$$

One should also keep in mind that there are several limitations with the internal shock model. The thickness of the shell ( $\frac{r}{\Gamma}$ ) may limit the maximum energy of the protons. Moreover, the relative kinetic energy between the colliding shells has to give the emission energy of GRBs. Hence, the radiation efficiency has to be high to attain the observed energy output during prompt emission of these sources. Also, the spectra observed by BATSE from some bright GRBs suggest at least within the same burst the peak photon energy distribution is narrow. This is hard to achieve within the internal shock model unless one invokes a strong bimodal distribution in the values of the bulk Lorentz factor.

## 5 Proton Spectrum in the External Shock Model

The expanding shells of GRBs push the external medium which results in external shocks. In [26] the authors proposed that thermalization of the spectrum of the GRB can be avoided by introducing a slight contamination of baryons within the original fireball. The baryon loading parameter is defined as

$$\Gamma = \frac{E_{tot}}{Mc^2} \tag{20}$$

where  $M$  is the total baryon mass and  $E_{tot}$  is the total energy of the photon-pair fireball. [35] (MLR) showed that for a certain range of values of  $\Gamma_0$  only a fraction of the initial energy is still in the form of radiation when the expanding fireball is optically thin. The rest of the energy gets converted into kinetic energy of the baryons. For high baryon loading the baryons can be accelerated such that almost all the initial fireball energy transforms into kinetic energy of the baryons. After an initial period of acceleration, the fireball expands freely. The energy in this phase is concentrated in a thin slab initially of roughly constant thickness  $\delta r \simeq r_0$ . After free expansion starts the shell thickness is given by [35]

$$\delta r = \begin{cases} \Gamma r_0 & r_s < r < r_b \\ r/\Gamma & r > r_b \end{cases} \tag{21}$$

where  $r_s$  is the radius where free expansion starts and later the shell starts expanding linearly with  $r$  when  $r > r_b$ . The baryons can radiate if their kinetic energy can be properly randomized either by collisions with the external interstellar medium (ISM) or with slower/faster portions of the relativistic flow itself [36]. Finally, the fireball shell is decelerated by the ISM. During the initial interaction of the fireball shell with the external medium a reverse shock propagates into the fireball to stop it. A prompt fireball collects  $1/\Gamma$  times its rest mass from the ISM by the time the fireball's radius attends the deceleration radius. The baryons

or cosmic rays can lose energy by photopion interactions  $p + \gamma \rightarrow \pi^0, \pi^+$  and synchrotron radiation inside the shell of thickness  $\delta r$ . We derive the cooling break energy and the maximum proton energy comparing the different time scale for the forward shock scenario. In the external shock model the expansion time scale at any time  $t$  is  $t'_{dyn} = \Gamma t$ . At the deceleration epoch it is  $\frac{r_{dec}}{c\Gamma_{dec}}$  where  $r_{dec}$  is the deceleration radius and  $\Gamma_{dec}$  is the Lorentz factor at that radius. This radius can be expressed as  $r_{dec}^{HL} \simeq (2.5 \times 10^{16} \text{cm})(E_{tot,52}/n)^{1/3}(\Gamma_{dec,2.5})^{-2/3}$  [20] and  $r_{dec}^{LL} \simeq (5.4 \times 10^{16} \text{cm})(E_{tot,50}/n)^{1/3}(\Gamma_{dec,1})^{-2/3}$  where  $E_{tot}$  is the total energy of a blast wave. The comoving magnetic field at the deceleration epoch is  $B'_{dec}{}^{HL} = c\Gamma_{dec}(32\pi n m_p \epsilon_B)^{1/2} = 39\Gamma_{dec,2.5}(n\epsilon_{B,-1})^{1/2} \text{G}$ ,  $B'_{dec}{}^{LL} = 1.23\Gamma_{dec,1}(n\epsilon_{B,-1})^{1/2} \text{G}$ .  $n \sim 1$  is particle number density of the ambient medium.

For interstellar medium (ISM) the radius of wind expansion at any time  $t$  measured in the source rest frame is ([37])

$$\begin{aligned} r^{HL}(t) &= 4 \times 10^{16} \left( E_{tot,52}/n \right)^{1/4} t_h^{1/4} \text{cm} \\ r^{LL}(t) &= 1.25 \times 10^{16} \left( E_{tot,50}/n \right)^{1/4} t_h^{1/4} \text{cm} \end{aligned} \quad (22)$$

The Lorentz factor decreases with time as follows

$$\begin{aligned} \Gamma^{HL}(t) &= 19.4 \left( E_{tot,52}/n \right)^{1/8} t_h^{-3/8} \\ \Gamma^{LL}(t) &= 11 \left( E_{tot,50}/n \right)^{1/8} t_h^{-3/8} \end{aligned} \quad (23)$$

where  $t_h$  is the time measured in the source rest frame in hours. We have used  $r = \Gamma^2 ct$ . The time dependent comoving magnetic field is

$$\begin{aligned} B'^{HL}(t) &= 7.5 G \epsilon_B^{1/2} E_{tot,52}^{1/8} n^{3/8} t_h^{-3/8} \\ B'^{LL}(t) &= 4.2 G \epsilon_B^{1/2} E_{tot,50}^{1/8} n^{3/8} t_h^{-3/8} \end{aligned} \quad (24)$$

From  $t'_{dyn} = t'_{syn}$ , the break energy in the proton spectrum of GRBs due to synchrotron cooling of protons is

$$\begin{aligned} E_{p,c,syn}^{HL} &= 2 \times 10^{22} E_{tot,52}^{-1/4} n^{-3/4} \epsilon_B^{-1} t_h^{-1/4} \text{eV} \\ E_{p,c,syn}^{LL} &= 6 \times 10^{22} E_{tot,50}^{-1/4} n^{-3/4} \epsilon_B^{-1} t_h^{-1/4} \text{eV} \end{aligned} \quad (25)$$

At the deceleration epoch this expression becomes

$$\begin{aligned} E_{p,c,syn}^{HL} &= 7.5 \times 10^{21} \frac{\Gamma_{dec,2.5}^{2/3}}{n\epsilon_{B,-1}} \left( \frac{E_{tot,52}}{n} \right)^{-1/3} \text{eV} \\ E_{p,c,syn}^{LL} &= 1.64 \times 10^{21} \frac{\Gamma_{dec,1}^{2/3}}{n\epsilon_{B,-1}} \left( \frac{E_{tot,50}}{n} \right)^{-1/3} \text{eV} \end{aligned} \quad (26)$$

$t'_{dyn} = t'_{p\gamma}$  gives

$$E_{p,c,p\gamma}^{HL,LL} = \frac{E_{pb}^{HL,LL}}{1.34} \left[ \frac{(1 + \alpha_1)}{f_0^{HL,LL}} \right]^{\frac{1}{(\alpha_1 - 1)}} \quad (27)$$



The time dependence of this cooling break energy is calculated below. The photon energy flux at the peak/break energy is proportional to  $t^{-1}, t^{-p/2}$  in the case of fast and slow cooling respectively. For  $p \sim 2$  the two cases are almost similar. This is also true for the luminosity of the low energy photons if the threshold energy of photo-pion production is below the peak energy. If the threshold energy is above the peak energy then the luminosity would be proportional to  $t^{-p/4-1/2}$  for both fast and slow cooling of electrons. The threshold energy condition for  $p\gamma$  interaction in the source rest frame gives  $E_{\gamma,peak}(t)E_{pb}(t) = 0.3\Gamma^2(t)GeV^2$ . If it is slow cooling  $E_{\gamma,peak}(t) \propto t^{-1/2}$  and in the case of fast cooling it is proportional to  $t^{-3/2}$ . If the threshold energy of  $p\gamma$  interaction is lower than the peak fluence energy in the afterglow photon spectrum then luminosity  $L(t) \propto t^{-1}, t^{-p/2}$  in the case of fast and slow cooling respectively. For  $p \sim 2$  we get  $L(t) \propto t^{-1}$  in both the cases. Considering the external medium to be ISM  $f_0^{HL,LL} \propto L(t)/(\Gamma^4(t)tE_{\gamma,peak}(t)) \propto t^0, t$  for slow and fast cooling respectively. The break energy due to  $p\gamma$  cooling in the source rest frame is proportional to  $t^{-1/4}, t^{-5/4}$  with  $\alpha_1 \approx 1.5$ , for slow and fast cooling respectively. The time dependence of the  $p\gamma$  cooling depends on several factors like the photon flux, the external medium (ISM or wind) and whether electrons cool slow or fast. For different underlying assumptions one gets different time dependence of the  $p\gamma$  cooling ([12, 17]). The cooling break energy in the proton spectrum is  $E'_{p,c} = \min[E'_{p,c,syn}, E'_{p,c,p\gamma}]$ . We compare the cooling and acceleration time scales to derive the maximum energy of protons.

$$\begin{aligned} E'_{p,max,syn}{}^{HL} &= 7 \times 10^{21} \frac{\Gamma_{dec,2.5}^{1/2}}{(n\epsilon_{B,-1})^{1/4}} eV \\ E'_{p,max,syn}{}^{LL} &= 4 \times 10^{20} \frac{\Gamma_{dec,1}^{1/2}}{(n\epsilon_{B,-1})^{1/4}} eV \end{aligned} \quad (28)$$

After the deceleration epoch the time dependent maximum energy obtained by comparing synchrotron cooling and acceleration time scales is

$$E'_{p,max,syn}{}^{HL} = \Gamma(t) \left[ \frac{3em_p^2 c^4}{\sigma_{p,T} B'^{HL}(t)} \right]^{0.5} = 6 \times 10^{20} \epsilon_B^{-1/4} E_{tot,52}^{1/16} n^{-5/16} t_h^{-3/16} eV \quad (29)$$

for  $\beta'_p \sim 1$ . The maximum energy of protons derived by comparing the acceleration and pion production time scales is

$$E'_{p,max,p\gamma}{}^{HL} = \Gamma(t) \left[ \frac{eB'^{HL}(t)}{2\pi} \frac{\Gamma(t)t(1+\alpha_1)}{f_0^{HL}} \left( \frac{E'_{pb}}{1.34} \right)^{\alpha_1-1} \right]^{1/\alpha_1} \quad (30)$$

At the deceleration epoch

$$E'_{p,max,p\gamma}{}^{HL} = \Gamma_{dec} \left[ \frac{eB'_{dec}{}^{HL} r_{dec}^{HL}(1+\alpha_1)}{2\pi \Gamma_{dec} f_0^{HL}} \left( \frac{E'_{pb}}{1.34} \right)^{\alpha_1-1} \right]^{1/\alpha_1} \quad (31)$$

for  $\alpha_1 = 1.5$

$$\begin{aligned} E'_{p,max,p\gamma}{}^{HL} &= 5 \times 10^{18} \left[ \frac{n\epsilon_{B,-1}}{(f_0^{HL})^2} \left( \frac{E_{tot,52}}{n} \right)^{2/3} \frac{(\Gamma_{dec,2.5})^{8/3}}{E_{\gamma,peak,MeV}} \right]^{1/3} eV \\ E'_{p,max,p\gamma}{}^{LL} &= 10^{18} \left[ \frac{n\epsilon_{B,-1}}{(f_0^{LL})^2} \left( \frac{E_{tot,50}}{n} \right)^{2/3} \frac{(\Gamma_{dec,1})^{8/3}}{E_{\gamma,peak,keV}} \right]^{1/3} eV \end{aligned} \quad (32)$$

From  $t'_{dyn} = t'_{acc}$  we get

$$\begin{aligned}
E_{p,max,dyn}^{HL,LL} &= \frac{eB'^{HL,LL}(t)c}{2\pi}\Gamma(t)^2t \\
E_{p,max,dyn}^{HL} &= 1.4 \times 10^{19} \epsilon_B^{1/2} (E_{tot,52}^3 n/t_h)^{1/8} eV \\
E_{p,max,dyn}^{LL} &= 2.5 \times 10^{18} \epsilon_B^{1/2} (E_{tot,50}^3 n/t_h)^{1/8} eV
\end{aligned} \tag{33}$$

At the deceleration epoch

$$\begin{aligned}
E_{p,max,dyn}^{HL,LL} &= \frac{eB'_{dec}{}^{HL}}{2\pi} r_{dec}^{HL} \\
E_{p,max,dyn}^{HL} &= 2 \times 10^{19} (n\epsilon_{B,-1})^{1/2} \left(\frac{E_{tot,52}}{n}\right)^{1/3} (\Gamma_{dec,2.5})^{1/3} eV \\
E_{p,max,dyn}^{LL} &= 1.5 \times 10^{18} (n\epsilon_{B,-1})^{1/2} \left(\frac{E_{tot,50}}{n}\right)^{1/3} (\Gamma_{dec,1})^{1/3} eV
\end{aligned} \tag{34}$$

We calculate  $E_{p,max}$  as discussed in the previous section. The protons lose energy as long as the cooling time scale is much shorter than the wind expansion time scale. For  $\epsilon_p \sim 1$  the mean Lorentz factor of the protons is roughly the Lorentz factor of the forward shock. The total number of protons increases as  $nr(t)^3 \propto t^{3/4}$  incase of ISM and as  $nr(t)^3 \propto r(t) \propto t^{1/2}$  for wind medium. The total energy carried by protons remains constant,  $\epsilon_p E_{tot} = N_p \Gamma(t)^2 m_p c^2 \propto t^0$ . The proton spectrum has been normalised as given in eqn.(15). It is important to discuss the difficulty with the external shock model. The particles (e,p) need to be thrown back to the external shock region by some magnetic field for their reacceleration. The magnetic field in the ISM is known to be low. For acceleration of the protons to very high energy in the external shock model the ambient magnetic field has to be more than its typical value in the ISM. It is not physically impossible that the ambient medium close to GRBs is more magnetized than the average ISM. Alternatively, magnetic field amplification may lead to acceleration of particles to very high energy. For discussions on particle acceleration in this way in the non relativistic regime one may see [38, 39].

## 6 Internal Shocks: Average Proton Flux from GRBs

We have used the broken power law luminosity distribution functions for HL GRBs [16].

$$S(L) = S_0 \left[ \left(\frac{L}{L_b}\right)^{\beta_1} + \left(\frac{L}{L_b}\right)^{\beta_2} \right]^{-1} \tag{35}$$

The break luminosity  $L_b = 10^{52}$  erg/sec for HL GRBs. The values of  $\beta_1, \beta_2$  are taken to be 0.65, 2.3. The star formation rate is ([21])

$$R_{GRB} = 23\rho_0 \frac{e^{3.4z}}{e^{3.4z} + 22.0} \tag{36}$$

and  $\rho_0 \sim 1$ . The diffuse proton flux can be calculated as follows

$$M_p^{ob}(L_\gamma, \Gamma, T_d, t_v, E_p^{ob}) = \int_0^{z_{max}} \frac{dN_p^{ob}(E_p^{ob})}{dE_p^{ob}} \frac{R_{GRB}(z)}{1+z} dV(z) \tag{37}$$

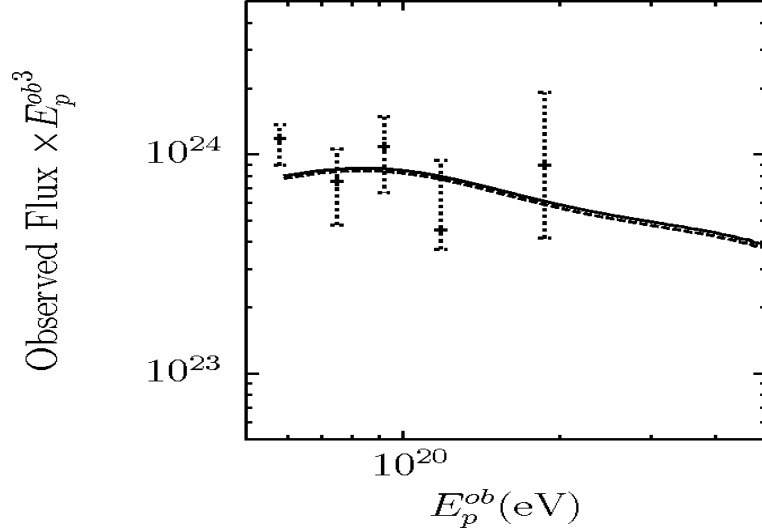


Figure 1: proton flux above 60EeV in  $eV^2 m^{-2} sec^{-1} sr^{-1}$  from HL GRBs using the internal shock model,  $z_{max} = 0.02$ ,  $\theta_a = 4^\circ, 10^\circ$  (solid line, dashed line). We have considered fast cooling of electrons and  $p = 2.3$  [33],  $\epsilon_p = 0.8$  and  $\epsilon_e = 0.1$ . The data points are from recent results of PA experiment [43]

$T_d$  is the duration of a burst and  $t_v$  is the variability time scale in the internal shock model. The isotropic energy emitted by low energy photons ( $E_\gamma = T_d L_\gamma$ ) is related to the total energy of a GRB

$$E_\gamma = \frac{\epsilon_e \eta_e}{1 + Y_e} E_{tot} \quad (38)$$

Amati-relation [40, 41] has been used to calculate the peak fluence energy in the low energy photon spectrum while using the internal shock model. We have averaged over all the relevant parameters ( $\Gamma$ ,  $L_\gamma$ ,  $T_d$ ,  $t_v$ ) as discussed in [22]. For the log normal distribution in Lorentz factor the peak is assumed to be at  $\log(\Gamma_m) = 2.6$  with standard deviation 0.3 for HL GRBs. The durations of the bursts are assumed to follow log normal distribution with the mean at  $\log(T_{d,m}) = 1.5$  with standard deviation 0.5. The mean of the log normal distribution in variability time is assumed to be at  $\log(t_{v,m}) = -1.5$  with standard deviation 0.3. In Fig.1. our calculated proton spectrum has been compared with PA data above 60EeV. If we increase the average deflection angle of the cosmic ray protons from  $4^\circ$  to  $10^\circ$  the proton flux does not change significantly.

## 7 External Shocks: Proton Flux from GRBs

In the external shock model we have calculated the proton flux from all GRBs using log normal distribution in total energy with the mean at  $\log(E_{tot,m,erg}) = 54$  and standard deviation 2 [42]. The distribution in the values of the Lorentz factor at the deceleration

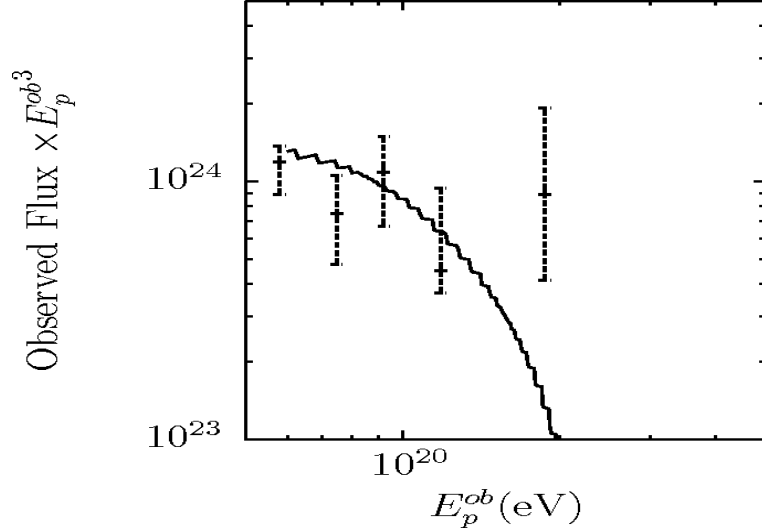


Figure 2: proton flux above 60EeV in  $eV^2 m^{-2} sec^{-1} sr^{-1}$  from HL GRBs using the external shock model at the deceleration epoch,  $z_{max} = 0.02$ ,  $\theta_a = 4^\circ$  as before also  $p = 2.3$  [33].  $\epsilon_p = 0.5$  and  $\epsilon_B = 0.3$ .

epoch is also assumed to be log normal with the mean 2.6 and standard deviation 0.3. The proton flux from all HL GRBs at the deceleration epoch is shown in Fig.2. We have used the particle number density in the ISM to be  $n = 1cm^{-3}$ . After the deceleration epoch the maximum energy of protons decreases with time and the chances of getting cosmic ray protons above 60 EeV becomes less. From LL GRBs we expect even lower cosmic ray flux than that from HL ones.

## 8 Maximum Energies of Protons:Internal vs External Shocks

In Fig.3. the three plots show how the maximum and cooling energies depend on the GRB parameters in the internal shock model. For  $\Gamma \sim 100$  the minimum of the maximum energies of protons is due to  $p\gamma$  cooling. As Lorentz factor increases the maximum energy of the protons is determined by the dynamical time scale. If the total energy of the low energy photons is varied synchrotron cooling of protons remains unaffected as long as the luminosity of a GRB remains constant. For  $\Gamma = 300$ ,  $t_v = 1sec$  and  $L_\gamma = 10^{51} eg/sec$  the dynamical timescale determines the maximum energy of the protons in the entire range of  $E_\gamma$  considered in our work. The maximum energy determined by the dynamical time scale is independent of the variability time of GRBs as shown in the third plot of Fig.3. For higher values of variability times of GRBs the rate of dynamical expansion determines the minimum of the maximum energies of protons. Fig.4. shows the various energies (maximum and cooling) in the case of external shocks. Unless Lorentz factor is nearly 1000,  $p\gamma$  cooling determines the

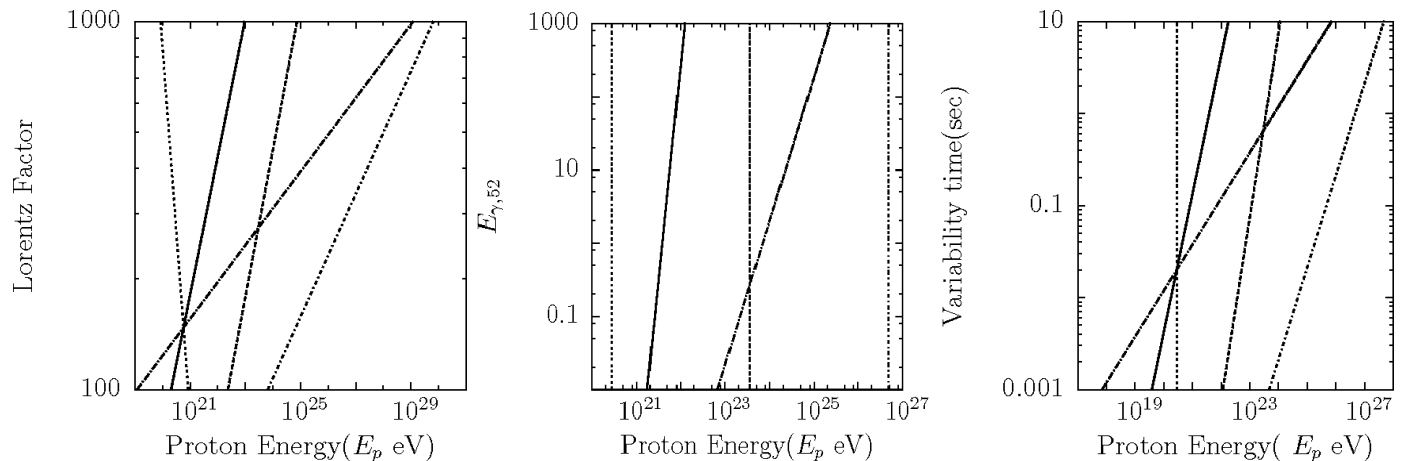


Figure 3: Internal Shock Model: First plot- total energy carried by low energy photons  $E_{\gamma,52} = 1$ ,  $t_v = 1sec$ ; second plot-  $\Gamma = 300$ ,  $t_v = 1sec$ ; third plot-  $\Gamma = 300$ ,  $E_{\gamma,52} = 1$ .  $E_{p,max,p\gamma}$  (solid line);  $E_{p,max,dyn}$  (dotted line);  $E_{p,max,syn}$  (dashed line);  $E_{p,c,p\gamma}$  (long dash dotted line);  $E_{p,c,syn}$  (small dash dotted line);  $\epsilon_p = 0.8$ ,  $\epsilon_e = 0.1$ ,  $L_\gamma = 10^{51}erg/sec$

maximum energies of protons.  $p\gamma$  cooling is more important in the case of external shocks than in internal shocks. We vary the total energy of the GRB, particle density of the medium and find  $p\gamma$  cooling gives the minimum of the maximum energies of potons. The cooling break energies are not important in case of external shocks as they are very high.

## 9 Conclusions

The leading theoretical models often used to explain emissions from GRBs are the internal and the external shock models. Within these models cosmic rays can be accelerated to extremely high energies inside these sources. Cosmic ray proton fluxes above 60 EeV have been calculated from GRBs distributed upto a redshift of 0.02 assuming distributions in the values of the relevant GRB parameters. The recent data from the Pierre Auger experiment is compared with our calculated proton fluxes. Our results show that GRBs can emit cosmic ray flux comparable to the PA data above 60EeV both in the internal and external shock models. In the internal shock model  $p\gamma$  cooling and the dynamical expansion time scale of the GRBs are important in determining the maximum energy of the protons while in the case of the external shock model  $p\gamma$  cooling determines the maximum energy of the shock accelerated protons.

## 10 Acknowledgement

I thank Bing Zhang for many helpful communications and to the anonymous referee for important suggestions.

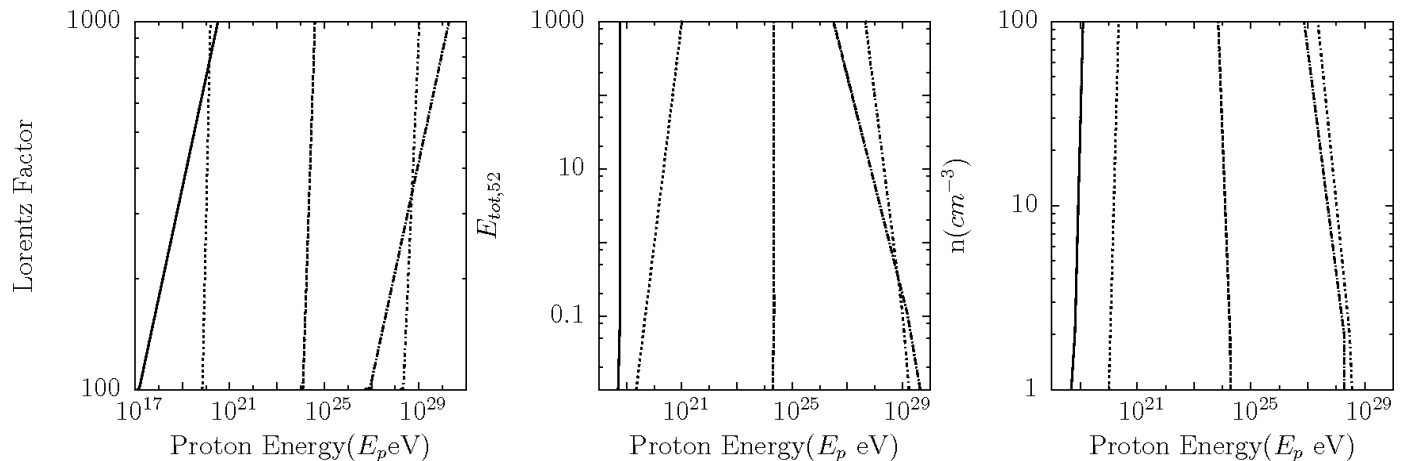


Figure 4: External Shock Model: First plot-  $E_{tot,52} = 1$ ,  $n = 1\text{cm}^{-3}$ ; second plot-  $\Gamma = 300$ ,  $n = 1\text{cm}^{-3}$ ; third plot-  $\Gamma = 300$ ,  $E_{tot,52} = 1$ ;  $\epsilon_B = 0.5$ ,  $\epsilon_p = 0.3$ . Different line styles used as in Fig.3.

## References

- [1] J. Abraham et al., Science **318**, 938 (2007).
- [2] D. J. Bird et al., ApJ **424**, 491 (1994).
- [3] N. Hayashida et al., AJ **120**, 2190 (2000).
- [4] K. Greisen, Phys. Rev. Lett. **16**, 748 (1966).
- [5] G. T. Zatsepin, & V. A. Kuzmin, JETP Lett. **4**, 78 (1966).
- [6] C. D. Dermer, arxiv:0711.2804.
- [7] J. Abraham et al., arxiv:0712.2843.
- [8] E. Waxman, ApJ **452**, L1 (1995).
- [9] E. Waxman, Lect. Notes Phys. **576**, 122 (2001).
- [10] M. Vietri, ApJ **453**, 883 (1995).
- [11] M. Vietri, ApJ **592**, 378 (2003).
- [12] X. Y. Wang, S. Razzaque and P. Mészáros, ApJ **677**, 432 (2007).
- [13] B. E. Cobb, C. D. Bailyn, P. G. van Dokkum and P. Natarajan, ApJ **645**, L113 (2006).
- [14] E. Pian et al., Nature **442**, 1011 (2006).

- [15] A. M. Soderberg et al., *Nature* **442**, 1014 (2006).
- [16] E. Liang et al., *ApJ* **662**, 1111 (2007).
- [17] K. Murase K., *PRD* **78**, 023005 (2008).
- [18] K. Dolag et al., *JCAP* **0501**, 009 (2005).
- [19] G. Sigl, F. Miniati & T. A. Ensslin, *Phys. Rev. D*, **70**, 043007 (2004).
- [20] B. Zhang & P. Mészáros, *IJMP A* **19**, 2385 (2004).
- [21] C. Porciani, & P. Madau, *ApJ* **548**, 522 (2001).
- [22] N. Gupta, B. Zhang, *Astropart. Phys.* **27**, 386 (2007); The log normal distribution functions used in this paper should have an extra factor of 0.43, we thank P. Bhattacharjee for finding this error.
- [23] J. Miralda-Escudé, & E. Waxman, *ApJ* **462**, L59 (1996).
- [24] E. Waxman, & J. Miralda-Escudé, *ApJ* **472**, L89 (1996).
- [25] T. Stanev et al, *Phys. Rev. D* **62**, 093005 (2000).
- [26] M. J. R. Rees, & P. Mészáros, *MNRAS* **258**, 41 (1992).
- [27] R. P. Pilla, & A. Loeb, *ApJ* **494**, L167 (1998).
- [28] P. C. Fragile et al., *Astropart. Phys.* **20**, 591 (2004).
- [29] P. Bhattacharjee, & N. Gupta, *Astropart. Phys.* **20**, 169 (2003).
- [30] S. Razzaque, P. Mészáros, & B. Zhang, *ApJ* **613**, 1072 (2004).
- [31] A. Pe’er, & E. Waxman, *ApJ* **613**, 448 (2004).
- [32] A. Pe’er, P. Mészáros, & M. J. Rees, *ApJ* **642**, 995 (2006).
- [33] N. Gupta, & B. Zhang, *MNRAS* **380**, 78 (2007).
- [34] B. Zhang, & P. Mészáros, *ApJ* **581**, 1236 (2002).
- [35] P. Mészáros, P. Laguna & M. J. Rees, *ApJ* **415**, 181 (1993).
- [36] P. Mészáros, & M. J. Rees, *ApJ* **405**, 278 (1993).
- [37] B. Zhang, & P. Mészáros, *ApJ* **559**, 110 (2001).
- [38] P. Blasi & E. Amato, 30th ICRC Merida, Mexico, 2007
- [39] P. Blasi, E. Amato, & D. Caprioli, *MNRAS* **375**, 1471 (2007).
- [40] L. Amati et al., *A&A* **390**, 81 (2002).

- [41] G. Ghirlanda G. et al., MNRAS Lett. **361**, 10G (2005).
- [42] E. Liang et al., ApJ **675**, 528L (2008).
- [43] J. R. T. De Mello Neto, arxiv:0712.3727.